

# Constraining simultaneously nuclear symmetry energy and neutron-proton effective mass splitting with nucleus giant resonances from a dynamical approach

Hai-Yun Kong,<sup>1,2</sup> Jun Xu\*,<sup>1</sup> Lie-Wen Chen,<sup>3,4</sup> Bao-An Li,<sup>5,6</sup> and Yu-Gang Ma<sup>1,7</sup>

<sup>1</sup>*Shanghai Institute of Applied Physics, Chinese Academy of Sciences, Shanghai 201800, China*

<sup>2</sup>*University of Chinese Academy of Sciences, Beijing 100049, China*

<sup>3</sup>*Department of Physics and Astronomy and Shanghai Key Laboratory for Particle Physics and Cosmology, Shanghai Jiao Tong University, Shanghai 200240, China*

<sup>4</sup>*Center of Theoretical Nuclear Physics, National Laboratory of Heavy Ion Accelerator, Lanzhou 730000, China*

<sup>5</sup>*Department of Physics and Astronomy, Texas A&M University-Commerce, Commerce, TX 75429-3011, USA*

<sup>6</sup>*Department of Applied Physics, Xi'an Jiao Tong University, Xi'an 710049, China*

<sup>7</sup>*Shanghai Tech University, Shanghai 200031, China*

(Dated: March 14, 2017)

With a newly improved isospin- and momentum-dependent interaction and an isospin-dependent Boltzmann-Uehling-Uhlenbeck transport model, we have investigated the effects of the slope parameter  $L$  of the nuclear symmetry energy and the isospin splitting of the nucleon effective mass  $m_{n-p}^* = (m_n^* - m_p^*)/m$  on the centroid energy of the isovector giant dipole resonance and the electric dipole polarizability in  $^{208}\text{Pb}$ . With the isoscalar nucleon effective mass  $m_s^* = 0.7m$  constrained by the empirical optical potential, we obtain a constraint of  $L = 64.29 \pm 11.84(\text{MeV})$  and  $m_{n-p}^* = (-0.019 \pm 0.090)\delta$ , with  $\delta$  being the isospin asymmetry of nuclear medium. With the isoscalar nucleon effective mass  $m_s^* = 0.84m$  extracted from the excitation energy of the isoscalar giant quadrupole resonance in  $^{208}\text{Pb}$ , we obtain a constraint of  $L = 53.85 \pm 10.29(\text{MeV})$  and  $m_{n-p}^* = (0.216 \pm 0.114)\delta$ .

PACS numbers: 24.30.Cz, 21.65.+f, 21.30.Fe, 24.10.Lx

## I. INTRODUCTION

One of the main tasks of nuclear physics is to understand the in-medium nuclear interactions and the equation of state (EoS) of nuclear matter. The uncertainties of the isospin-dependent part of the EoS, i.e., the nuclear symmetry energy ( $E_{\text{sym}}$ ), has hampered our accurate understanding of nuclear matter properties, while it has important ramifications in heavy-ion reactions, astrophysics, and nuclear structures [1–8]. Thanks to the great efforts made by nuclear physicists in the past decade, a more stringent constraint on  $E_{\text{sym}}$  at subsaturation densities has been obtained from various analysis, with the slope parameter of the nuclear symmetry energy so far constrained within  $L = 60 \pm 20 \text{ MeV}$  [9–11], although further verifications are still needed. On the other hand, the in-medium isospin splitting of the nucleon effective mass  $m_{n-p}^* = (m_n^* - m_p^*)/m$  has become a hot topic recently. Compared to the bare nucleon mass in free space, the in-medium nucleon effective mass comes from the momentum-dependent potential in non-relativistic models (see, e.g., Chapter 3 of Ref. [7]). The isospin splitting of the in-medium nucleon effective mass is thus related to the momentum dependence of the symmetry potential in non-relativistic models [12]. It has been found that the isospin splitting of the nucleon effective mass is as important as the nuclear symmetry energy in understanding the isospin dynamics in nuclear reactions [13–19], and has

ramifications in the thermodynamic properties of isospin asymmetric nuclear matter as well [20, 21]. Moreover, the neutron-proton effective mass splitting is actually inter-related to the nuclear symmetry energy through the Hugenholtz-Van Hove theorem [10, 22]. For a recent review on the isospin splitting of the nucleon effective mass, we refer the reader to Ref. [23].

Giant resonances of nuclei serve as a useful probe of nuclear interactions and the EoS of nuclear matter at subsaturation densities. The studies on giant resonances mainly follow two methods, i.e., the random-phase approximation and the transport model calculations. As a breathing oscillation mode in the radial direction of a nucleus, the isoscalar giant monopole resonance (GMR) is a good probe of the incompressibility of nuclear matter [24–28], while the isoscalar giant quadrupole resonance (ISGQR), an oscillation mode with quadrupole deformation of a nucleus, has been found to be much affected by the isoscalar nucleon effective mass  $m_s^*$  [29–34]. On the other hand, the isovector giant dipole resonance (IVGDR) and the pygmy dipole resonance (PDR), with the former an oscillation mode between the centers of mass of neutrons and protons and the latter that between the neutron skin and the nucleus core, are valuable probes of the nuclear symmetry energy at subsaturation densities [35–49]. Since the nuclear symmetry energy acts as a restoring force for the IVGDR, the main frequency of the IVGDR oscillation, i.e., the centroid energy  $E_{-1}$ , is related to  $E_{\text{sym}}$  at subsaturation densities or its slope parameter  $L$  at the saturation density [36, 45, 49]. The electric dipole polarizability  $\alpha_D$  has a strong correlation with the neutron skin thickness  $\Delta r_{np}$  [38, 49], and  $\alpha_D$  times  $E_{\text{sym}}$  at

\*corresponding author: xujun@sinap.ac.cn

the saturation density shows a good linear dependence on  $L$  [44, 47, 48]. It was argued that the accurate knowledge of  $\alpha_D$  and  $\Delta r_{np}$  can help constrain significantly the nuclear symmetry energy at subsaturation densities [40]. The effect of the neutron-proton effective mass splitting on the IVGDR properties was realized only recently [34]. It is also worth mentioning that the dynamical isovector dipole collective motion in fusion reactions could be a probe of the nuclear symmetry energy as well from transport model studies [50–55].

Recently we have improved our isospin- and momentum-dependent interaction (MDI) [56, 57], which was previously extensively used in the studies of thermodynamic properties of nuclear matter, dynamics of nuclear reactions, and properties of compact stars (see Ref. [58] for a review). In the improved isospin- and momentum-dependent interaction (ImMDI) [21], the momentum dependence of the mean-field potential has been fitted to that extracted from proton-nucleus scatterings up to the nucleon kinetic energy of about 1 GeV, and more isovector parameters are further introduced so that the density dependence of the symmetry energy and the momentum dependence of the symmetry potential, or equivalently, the isospin splitting of the nucleon effective mass, can be mimicked separately. In the present study, we are going to investigate the effect of the nuclear symmetry energy and the neutron-proton effective mass splitting on the centroid energy  $E_{-1}$  of IVGDR as well as the electric dipole polarizability  $\alpha_D$ , by employing the ImMDI interaction together with the isospin-dependent Boltzmann-Uehling-Uhlenbeck (IBUU) transport model. With the experimental data of  $E_{-1}$  and  $\alpha_D$  from the IVGDR in  $^{208}\text{Pb}$  available [39, 47, 59], we are able to constrain both the slope parameter of the symmetry energy and the isospin splitting of the nucleon effective mass, once the isoscalar nucleon effective mass is well determined. Section II gives a brief introduction to the ImMDI interaction and the necessary formalisms for IVGDR. Detailed studies on the extraction of  $m_s^*$  and the constraint on  $L$  and  $m_{n-p}^*$  from IVGDR are presented in Sec. III. We conclude in Sec. IV.

## II. THEORY

### A. An improved isospin- and momentum-dependent interaction

The potential energy density functional in the asymmetric nuclear matter with isospin asymmetry  $\delta$  and nucleon number density  $\rho$  from the ImMDI interaction can

be expressed as [21, 56]

$$V(\rho, \delta) = \frac{A_u \rho_n \rho_p}{\rho_0} + \frac{A_l}{2\rho_0} (\rho_n^2 + \rho_p^2) + \frac{B}{\sigma + 1} \frac{\rho^{\sigma+1}}{\rho_0^\sigma} \\ \times (1 - x\delta^2) + \frac{1}{\rho_0} \sum_{\tau, \tau'} C_{\tau, \tau'} \\ \times \int \int d^3p d^3p' \frac{f_\tau(\vec{r}, \vec{p}) f_{\tau'}(\vec{r}, \vec{p}')}{1 + (\vec{p} - \vec{p}')^2 / \Lambda^2}. \quad (1)$$

The single-particle potential of a nucleon with isospin  $\tau$  and momentum  $\vec{p}$  in the asymmetric nuclear matter with the isospin asymmetry  $\delta$  and nucleon number density  $\rho$  can be expressed as

$$U_\tau(\rho, \delta, \vec{p}) = A_u \frac{\rho_{-\tau}}{\rho_0} + A_l \frac{\rho_\tau}{\rho_0} \\ + B \left( \frac{\rho}{\rho_0} \right)^\sigma (1 - x\delta^2) - 4\tau x \frac{B}{\sigma + 1} \frac{\rho^{\sigma-1}}{\rho_0^\sigma} \delta \rho_{-\tau} \\ + \frac{2C_l}{\rho_0} \int d^3p' \frac{f_\tau(\vec{r}, \vec{p}')}{1 + (\vec{p} - \vec{p}')^2 / \Lambda^2} \\ + \frac{2C_u}{\rho_0} \int d^3p' \frac{f_{-\tau}(\vec{r}, \vec{p}')}{1 + (\vec{p} - \vec{p}')^2 / \Lambda^2}. \quad (2)$$

In the above,  $\rho_n$  and  $\rho_p$  are the number density of neutrons and protons,  $\rho_0$  is the saturation density, and  $\delta = (\rho_n - \rho_p)/\rho$  is the isospin asymmetry.  $f_\tau(\vec{r}, \vec{p})$  is the phase-space distribution function with  $\tau = 1(-1)$  being the isospin label of neutrons (protons). The potential energy density of Eq. (1) can be derived based on the Hartree-Fock calculation from an effective interaction with a zero-range density-dependent term and a finite-range Yukawa-type term [60].

In the ImMDI interaction [21], the isovector parameters  $x$ ,  $y$ , and  $z$  are introduced to vary respectively the slope parameter of the symmetry energy, the momentum dependence of the symmetry potential or the neutron-proton effective mass splitting, and the value of the symmetry energy at the saturation density, via the following relations

$$A_l(x, y) = A_0 + y + x \frac{2B}{\sigma + 1}, \\ A_u(x, y) = A_0 - y - x \frac{2B}{\sigma + 1}, \\ C_l(y, z) = C_{l0} - 2(y - 2z) \frac{p_f^2}{\Lambda^2 \ln[(4p_f^2 + \Lambda^2)/\Lambda^2]}, \\ C_u(y, z) = C_{u0} + 2(y - 2z) \frac{p_f^2}{\Lambda^2 \ln[(4p_f^2 + \Lambda^2)/\Lambda^2]}, \quad (3)$$

where  $p_f = \hbar(3\pi^2\rho_0/2)^{1/3}$  is the nucleon Fermi momentum in symmetric nuclear matter at the saturation density. We set  $z = 0$  all through the manuscript. The values of the parameters  $A_0$ ,  $B$ ,  $C_{u0}$ ,  $C_{l0}$ ,  $\sigma$ ,  $\Lambda$ ,  $x$ , and  $y$  can be fitted or solved from the saturation density  $\rho_0$ , the binding energy  $E_0$  at  $\rho_0$ , the incompressibility  $K_0$ , the

mean-field potential  $U_0^\infty$  at infinitely large nucleon momentum at  $\rho_0$ , the isoscalar nucleon effective mass  $m_s^*$  at  $\rho_0$ , the symmetry energy  $E_{sym}$  and its slope parameter  $L$  at  $\rho_0$ , and the isovector nucleon effective mass  $m_v^*$  at  $\rho_0$ , as detailed in APPENDIX A.

### B. Isovector giant dipole resonance

The isovector giant dipole resonance (IVGDR) is a collective vibration of protons against neutrons, with the isovector dipole operator defined as

$$\hat{D} = \frac{NZ}{A} \hat{X}, \quad (4)$$

where  $N$ ,  $Z$ , and  $A = N + Z$  are the number of neutrons, protons, and the mass number of the nucleus, respectively, and  $\hat{X}$  is the distance between the centers of mass of protons and neutrons in the nucleus. The strength function of IVGDR can be calculated from the isovector dipole moment via

$$S(E) = \frac{-\text{Im}[\tilde{D}(\omega)]}{\pi\eta}, \quad (5)$$

where  $\tilde{D}(\omega) = \int_{t_0}^{t_{max}} D(t) e^{i\omega t} dt$  is the fourier transformation of the isovector dipole moment with  $E = \hbar\omega$ . In order to initialize the isovector dipole oscillation, the initial momenta of protons and neutrons are given a perturbation in the opposite direction according to [61]

$$p_i \rightarrow \begin{cases} p_i - \eta \frac{N}{A} & (\text{protons}) \\ p_i + \eta \frac{N}{A} & (\text{neutrons}) \end{cases}, \quad (6)$$

with  $p_i$  being the momentum of the  $i$ th nucleon along  $\hat{X}$ , and the perturbation parameter  $\eta = 25$  MeV/c used in the present study. One sees that a larger  $\eta$  leads to a larger amplitude of the oscillation  $D(t)$ , while the strength function  $S(E)$  is independent of  $\eta$  as the amplitude is cancelled from the denominator. Once the strength function of IVGDR is obtained, the moments of the strength function can be calculated from

$$m_k = \int_0^\infty dE E^k S(E). \quad (7)$$

Both the centroid energy and the electric dipole polarizability can be measured from photoabsorption experiments. The centroid energy, corresponding to the peak energy in the photoabsorption energy spectrum, is the main frequency of IVGDR. The electric dipole polarizability, characterizing the response of the nucleus to the external electric field, is related to the photoabsorption cross section  $\sigma_f$  via [39]

$$\alpha_D = \frac{\hbar c}{2\pi^2} \int \frac{\sigma_f}{\omega^2} d\omega. \quad (8)$$

Since both the strength function  $S(E)$  and the photoabsorption cross section  $\sigma_f$  are related to the energy spectrum of the excited states in the nucleus, the centroid energy and the electric dipole polarizability can be expressed in terms of the moments  $m_k$  of the strength function as

$$E_{-1} = \sqrt{m_1/m_{-1}} \quad (9)$$

and

$$\alpha_D = 2e^2 m_{-1}. \quad (10)$$

We note that the relation between  $\alpha_D$  and  $m_{-1}$  is different from that in Ref. [34], because we only consider one-dimensional oscillation, and the definition of the isovector giant dipole operator is different from that used in Ref. [34] based on a random-phase approximation approach.

In the following calculations, we fit the time evolution of the isovector giant dipole moment with the function

$$D(t) = a \sin(bt) e^{-ct}, \quad (11)$$

where  $a$ ,  $b$ , and  $c$  are fitting constants characterizing the amplitude, the frequency, and the damping time of IVGDR, respectively. With the help of Eq. (11), the strength function  $S(E)$ , the moments of the strength function  $m_{-1}$  and  $m_1$ , the centroid energy  $E_{-1}$  of IVGDR, and the electric dipole polarizability  $\alpha_D$  can be expressed analytically in terms of the fitting constants respectively as

$$\begin{aligned} S(E) &= \frac{-ac}{2\pi\eta} \left[ \frac{1}{c^2 + (b + \frac{E}{\hbar})^2} - \frac{1}{c^2 + (b - \frac{E}{\hbar})^2} \right], \\ m_{-1} &= \frac{-ab}{2\eta(b^2 + c^2)}, \\ m_1 &= \frac{-ab}{2\eta}, \\ E_{-1} &= \sqrt{m_1/m_{-1}} = \sqrt{b^2 + c^2}, \\ \alpha_D &= 2e^2 m_{-1} = \frac{-2e^2 ab}{2\eta(b^2 + c^2)}. \end{aligned} \quad (12)$$

### III. RESULTS AND DISCUSSIONS

In the following study, we employ the IBUU transport model together with the ImMDI interaction to investigate the giant resonances of nuclei. The positions of the projectile and target in the IBUU transport model are fixed, i.e., with zero beam energy. The initial density distribution is sampled according to that generated from Skyrme-Hartree-Fock calculations with the same physics quantities used in the ImMDI interaction, such as  $L$ ,  $m_v^*$ , etc., listed in Table I. The initial nucleon momentum is sampled accordingly to the local density from the Thomas-Fermi approximation. We generate events

from 40 runs with each run 200 test particles. Since the oscillation generally lasts for hundreds of fm/c, in order to improve the stability in the calculation with the momentum-dependent mean-field potential, we use the nuclear matter approximation in the real calculation by taking the phase-space distribution function as  $f_\tau(\vec{r}, \vec{p}) = \frac{2}{h^3} \Theta(p_{f_\tau} - p)$  and using the analytical expression (Eqs. (2) and (A.23)) for the momentum-dependent mean-field potential. This is similar to the spirit of the Thomas-Fermi approximation in the case that the vibration compared to the stable distribution is small. With this treatment, we found that up to  $t = 500$  fm/c only about 17% of the total nucleons become free particles.

### A. Extract the isoscalar nucleon effective mass

We first extract the isoscalar nucleon effective mass from the optical potential. The single-particle potentials in symmetric nuclear nuclear matter at the saturation density, with different values of the isoscalar nucleon effective mass  $m_s^*$  but same other isoscalar properties of the nuclear interaction, are displayed in Fig. 1. We can see that only the parameter set that leads to  $m_s^* = 0.7m$ , with  $m$  being the nucleon mass in free space, can describe reasonably well the real part of the optical potential extracted from proton-nucleus scatterings by Hama et al. [62, 63].

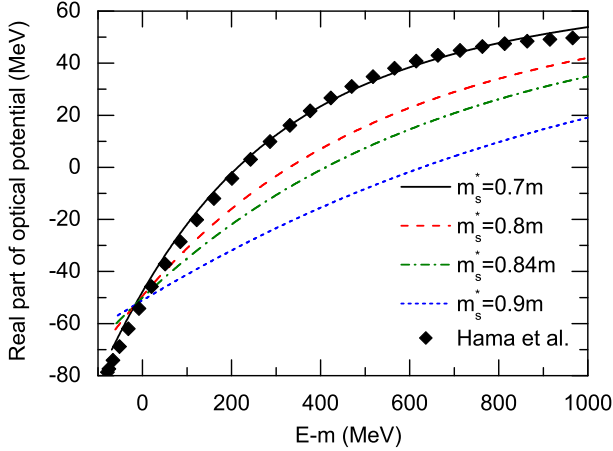


FIG. 1: (Color online) Single-particle potentials in symmetric nuclear nuclear matter at the saturation density as a function of the nucleon energy subtracted by the nucleon rest mass from the ImMDI interaction with different isoscalar nucleon effective mass  $m_s^*$ . The real part of the optical potential extracted from proton-nucleus scatterings by Hama et al. [62, 63] is shown by scatters for comparison.

Next, we extract the value of  $m_s^*$  from the isoscalar giant quadrupole resonance (ISGQR) in  $^{208}\text{Pb}$ , with the

operator written as

$$\hat{Q} = \sum_{i=1}^A r_i^2 Y_{20}(\hat{r}_i) = \sum_{i=1}^A \sqrt{\frac{5}{16\pi}} (3z_i^2 - r_i^2), \quad (13)$$

where  $r_i$  and  $z_i$  are respectively the radial and  $z$ -direction coordinate of the  $i$ th nucleon, and  $Y_{20}$  is the spherical harmonic function. Noticing that the following scaling relation in the ISGQR is observed (see, e.g., Ref. [64])

$$\begin{cases} x \rightarrow x/\lambda \\ y \rightarrow y/\lambda \\ z \rightarrow \lambda^2 z \end{cases} \begin{cases} p_x \rightarrow \lambda p_x \\ p_y \rightarrow \lambda p_y \\ p_z \rightarrow p_z/\lambda^2 \end{cases}, \quad (14)$$

we choose  $\lambda = 1.1$  in our simulation to initialize the oscillation. The value of  $\lambda$  is close to 1 corresponding to a small vibration with respect to the equilibrium distribution. Again, we found that the value of  $\lambda$  only affects the amplitude but has almost no effect on the frequency of ISGQR. The time evolution of the isoscalar giant quadrupole moment, with different values of the isoscalar nucleon effective mass but same other isoscalar properties of nuclear interaction, is displayed in the left panel of Fig. 2. It is seen that a smaller isoscalar nucleon effective mass  $m_s^*$  leads to a larger frequency of the oscillation. From the Fourier transformation of  $Q(t)$ , the linear correlation between the isoscalar nucleon effective mass  $m_s^*$  and the excitation energy of ISGQR is observed in the right panel of Fig. 2. It is found that the result from the isoscalar nucleon effective mass  $m_s^* = 0.84m$  reproduces best the excitation energy  $E_x = 10.9 \pm 0.1$  MeV of ISGQR in  $^{208}\text{Pb}$  extracted from  $\alpha$ -nucleus scattering experiments [65].

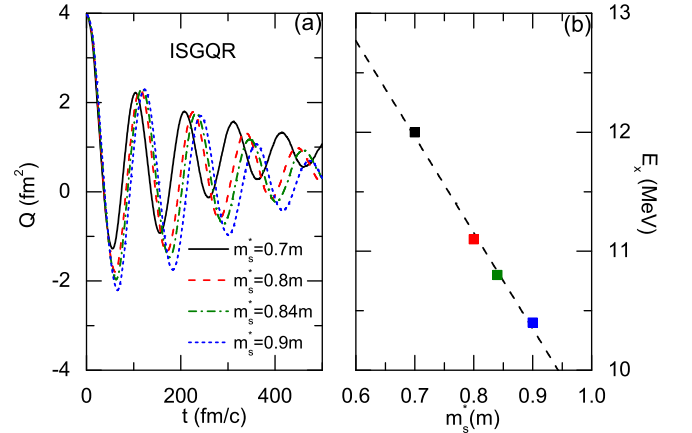


FIG. 2: (Color online) The time evolution of the isoscalar giant quadrupole moment in  $^{208}\text{Pb}$  (a) and the correlation between the corresponding excitation energy  $E_x$  and the isoscalar nucleon effective mass  $m_s^*$  (b).

The different values of the isoscalar effective mass  $m_s^*$  extracted from the optical potential and from the excitation energy of ISGQR in  $^{208}\text{Pb}$  represent the theoretical

TABLE I: The physics quantities and the corresponding parameters for the ImMDI interaction as well as the results from the IVGDR in  $^{208}\text{Pb}$ .

	Set I(a)	Set I(b)	Set I(c)	Set II(a)	Set II(b)	Set II(c)
$A_0$ (MeV)	-66.963	-66.963	-66.963	-96.799	-96.799	-96.799
$B$ (MeV)	141.963	141.963	141.963	171.799	171.799	171.799
$C_{u0}$ (MeV)	-99.70	-99.70	-99.70	-90.19	-90.19	-90.19
$C_{l0}$ (MeV)	-60.49	-60.49	-60.49	-50.03	-50.03	-50.03
$\sigma$	1.2652	1.2652	1.2652	1.2704	1.2704	1.2704
$\Lambda$ ( $p_f$ )	2.424	2.424	2.424	3.984	3.984	3.984
$x$	0	1	1	0	1	1
$y$ (MeV)	-115	-115	115	-115	-115	115
$\rho_0$ ( $\text{fm}^{-3}$ )	0.16	0.16	0.16	0.16	0.16	0.16
$E_0(\rho_0)$ (MeV)	-16	-16	-16	-16	-16	-16
$K_0$ (MeV)	230	230	230	230	230	230
$U_0^\infty$ (MeV)	75	75	75	75	75	75
$m_s^*$ ( $m$ )	0.7	0.7	0.7	0.84	0.84	0.84
$E_{sym}(\rho_0)$ (MeV)	32.5	32.5	32.5	32.5	32.5	32.5
$L$ (MeV)	58.57	8.70	60.00	72.63	11.24	36.03
$m_v^*$ ( $m$ )	0.537	0.537	0.853	0.712	0.712	0.928
$a$ (fm)	-28.13 $\pm$ 0.33	-27.16 $\pm$ 0.25	-19.55 $\pm$ 0.14	-24.30 $\pm$ 0.21	-22.69 $\pm$ 0.21	-19.34 $\pm$ 0.16
$b$ ( $\text{fm}^{-1}$ )	0.0782 $\pm$ 0.0001	0.0883 $\pm$ 0.0001	0.0614 $\pm$ 0.0001	0.0662 $\pm$ 0.0001	0.0760 $\pm$ 0.0001	0.0640 $\pm$ 0.0001
$c$ ( $\text{fm}^{-1}$ )	0.0075 $\pm$ 0.0001	0.0099 $\pm$ 0.0001	0.0040 $\pm$ 0.0001	0.0052 $\pm$ 0.0001	0.0075 $\pm$ 0.0001	0.0054 $\pm$ 0.0001
$E_{-1}$ (MeV)	15.50 $\pm$ 0.0001	17.53 $\pm$ 0.0001	12.13 $\pm$ 0.0001	13.10 $\pm$ 0.0001	15.06 $\pm$ 0.0001	12.68 $\pm$ 0.0001
$\alpha_D$ ( $\text{fm}^3$ )	20.5 $\pm$ 0.2	17.5 $\pm$ 0.2	18.3 $\pm$ 0.1	21.0 $\pm$ 0.2	17.0 $\pm$ 0.2	17.3 $\pm$ 0.1

uncertainties in the present study. In the following study, we will thus employ the parameter Set I and Set II that lead respectively to  $m_s^* = 0.7m$  and  $0.84m$  together with different combinations of the isovector parameters  $x$  and  $y$  to study the isovector giant dipole resonances of nuclei. The values of the parameters and the corresponding physics quantities are detailed in Table I.

### B. Constrain the symmetry energy and the neutron-proton effective mass splitting

We first employ the parameter Set I with  $m_s^* = 0.7m$ , which is able to reproduce the empirical optical potential as shown in Fig. 1, to study the properties of the IVGDR in  $^{208}\text{Pb}$ . Three different parameter sets, with different combinations of the slope parameter  $L$  of the symmetry energy and the isovector effective mass  $m_v^*$  detailed as Set I(a), Set I (b), and Set I(c) in Table I, are employed in the study. The initial momenta of neutrons and protons are modified with the perturbation parameter  $\eta$  as detailed in Sec. IIB. The oscillation amplitude is proportional to  $\eta$  while its frequency is found to be insensitive to the choice of  $\eta$ . The resulting time evolution of the isovector dipole moment is displayed in the left panel of Fig. 3. One sees that the time evolution of  $D(t)$  follows a good damping oscillation mode as in Eq. (11). In order to avoid oscillation in the Fourier transformation due to the finite  $t_{max}$

in the transport model calculation, a damping factor of  $\exp(-\frac{\gamma t}{2\hbar})$  with the width  $\gamma = 2$  MeV is multiplied to the isovector dipole moment  $D(t)$  in calculating the strength function  $S(E)$  from Eq. (5) as in Ref. [61]. This slightly affects the damping coefficient  $c$  in Eq. (11) but has very small effects on the final results as can be seen from the analytical formulae of Eq. (12). The resulting strength functions from the numerical Fourier transformation is displayed in the right panel of Fig. 3. It is seen that with a softer symmetry energy (Set I(b)), the main frequency, i.e., the centroid energy in the IVGDR, is larger, due to the larger symmetry energy at subsaturation densities acting as a stronger restoring force. On the other hand, the centroid energy is sensitive to the isovector nucleon effective mass as well, with a larger isovector effective mass (Set I(c)) leading to a smaller centroid energy of IVGDR. This could be understood since the oscillation frequency is smaller with a larger reduced mass of the system, with the latter attributed to the larger isovector effective mass once the isoscalar effective mass is fixed.

The constants  $a$ ,  $b$ , and  $c$  can be obtained from fitting the isovector dipole moment  $D(t)$  according to Eq. (11), and their detailed values for the three parameter sets are listed in Table I. The resulting centroid energy  $E_{-1}$  and the electric dipole polarizability  $\alpha_D$  calculated analytical according to Eq. (12) are also listed in Table I. It is seen that for a given isovector effective mass  $m_v^*$ , a larger slope parameter  $L$  leads to a smaller centroid energy  $E_{-1}$  and



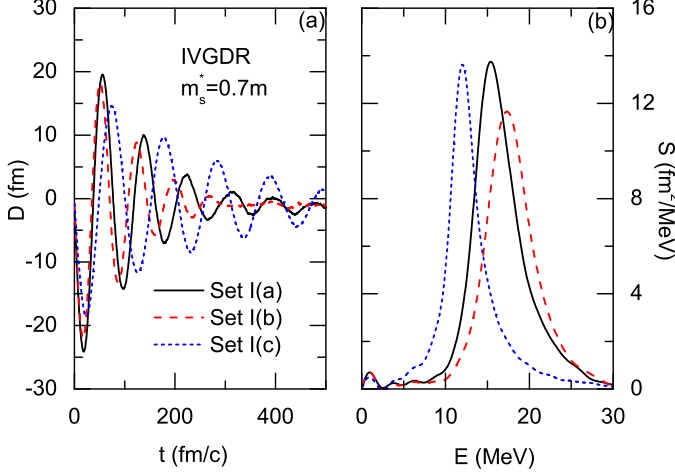


FIG. 3: (Color online) The time evolution of the isovector giant dipole moment (a) and the corresponding strength function (b) in  $^{208}\text{Pb}$  with  $m_s^* = 0.7m$ .

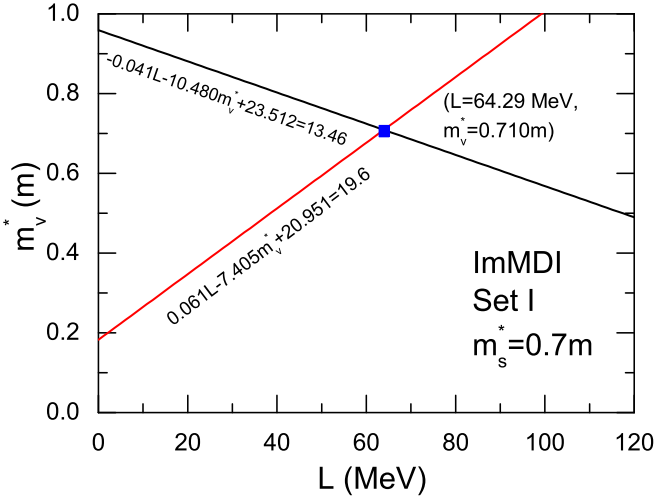


FIG. 4: (Color online) The linear relations between the symmetry energy slope parameter  $L$  as well as the isovector nucleon effective mass  $m_v^*$  and the centroid energy  $E_{-1}$  as well as the electric dipole polarizability  $\alpha_D$  from the IVGDR in  $^{208}\text{Pb}$ , respectively, with the isoscalar nucleon effective mass  $m_s^* = 0.7m$ .

a larger electric dipole polarizability  $\alpha_D$ . Analogously, for a given slope parameter  $L$ , a larger isovector effective mass  $m_v^*$  leads to a smaller centroid energy  $E_{-1}$  and a smaller electric dipole polarizability  $\alpha_D$ . The rigorous tool to treat such a problem of multiple experimental results with multiple parameters is the Bayesian framework [66–69], which is beyond the scope of the present study. On the other hand, we found both  $E_{-1}$  and  $\alpha_D$  are linearly correlated with  $L$  and  $m_v^*$ , and the corresponding relations based on our transport calculations turns out to

be

$$\begin{cases} -0.041L - 10.480m_v^* + 23.512 = E_{-1}, \\ 0.061L - 7.405m_v^* + 20.951 = \alpha_D, \end{cases} \quad (15)$$

with  $L$  in MeV,  $m_v^*$  in  $m$ ,  $E_{-1}$  in MeV, and  $\alpha_D$  in fm<sup>3</sup>. The centroid energy of the IVGDR in  $^{208}\text{Pb}$  obtained experimentally from the photoabsorption measurement is  $E_{-1} = 13.46$  MeV [59], while the electric dipole polarizability is  $\alpha_D = 19.6 \pm 0.6$  fm<sup>3</sup> measured from photoabsorption cross section by Tamii et al. [39] and with further correction by subtracting quasideuteron excitations [47]. With the above experimental data available, the constraints on the slope parameter  $L$  and the isovector effective mass can be solved from Eq. (15) as

$$L = 64.29 \pm 11.84 \text{ (MeV)}, \quad (16)$$

$$m_v^*/m = 0.710 \pm 0.046, \quad (17)$$

where the error bars, which originate from the fitting and the statistical error of  $a$ ,  $b$ , and  $c$  listed in Table I, are calculated from the error transfer. We found that the ImMDI parameterization with the mean values of  $L$  and  $m_v^*$  in Eq. (16) gives very close results of  $E_{-1}$  and  $\alpha_D$  compared with the experimental data, justifying the linear relation of Eq. (15). The corresponding isospin splitting of the nucleon effective mass deduced from Eq. (A.35) is

$$(m_n^* - m_p^*)/m = (-0.019 \pm 0.090)\delta. \quad (18)$$

The above constraint is, however, different from that obtained by analyzing nucleon-nucleus scattering data within an isospin-dependent optical model [70].

Next, we choose the isoscalar nucleon effective mass to be  $m_s^* = 0.84m$  while keeping other physics quantities the same in the ImMDI parameterization, and the resulting parameter sets are listed as Set II(a), Set II(b), and Set II(c) in Table I with different combinations of the parameter  $L$  of the symmetry energy and the isovector nucleon effective mass  $m_v^*$ . With the same calculation method, the time evolution of the isovector dipole moment in  $^{208}\text{Pb}$  and the corresponding strength function are displayed respectively in the left and right panel of Fig. 5. With  $a$ ,  $b$ , and  $c$  fitted by Eq. (11), and the analytical results of the centroid energy  $E_{-1}$  and the electric dipole polarizability  $\alpha_D$  obtained according to Eq. (12), we can get the similar linear relation from transport calculations as

$$\begin{cases} -0.032L - 7.346m_v^* + 20.651 = E_{-1}, \\ 0.065L - 6.368m_v^* + 20.845 = \alpha_D. \end{cases} \quad (19)$$

With the available experimental data of  $E_{-1}$  and  $\alpha_D$ , the slope parameter  $L$  of the symmetry energy and the isovector nucleon effective mass from the constraint of the ISQGR and the IVGDR in  $^{208}\text{Pb}$  are

$$L = 53.85 \pm 10.29 \text{ (MeV)}, \quad (20)$$

$$m_v^*/m = 0.744 \pm 0.045. \quad (21)$$

Again, we found that the mean values of  $L$  and  $m_v^*$  reproduce very well the experimental results of  $E_{-1}$  and  $\alpha_D$  within the statistical error based on our transport model calculations, justifying the linear relation of Eq. (19). The corresponding neutron-proton effective mass splitting deduced from Eq. (A.35) is thus

$$(m_n^* - m_p^*)/m = (0.216 \pm 0.114)\delta. \quad (22)$$

The constraint from both ISGQR and IVGDR on the neutron-proton effective mass splitting is consistent with that obtained in Ref. [70].

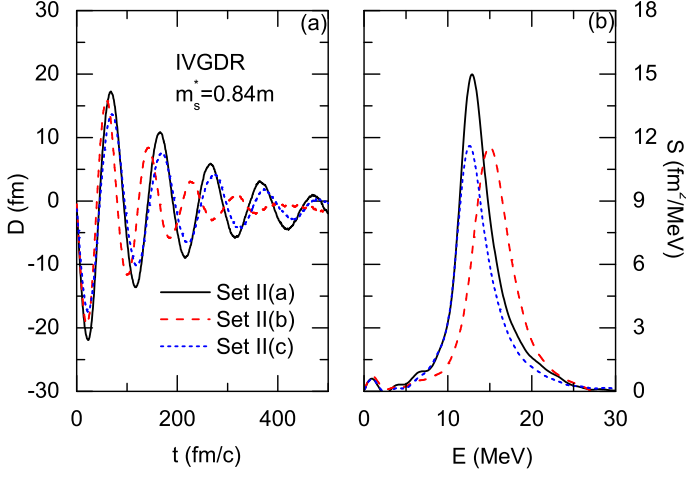


FIG. 5: (Color online) Same as Fig. 3 but with the isoscalar nucleon effective mass  $m_s^* = 0.84m$ .

#### IV. CONCLUSIONS

Based on an improved isospin- and momentum-dependent interaction (ImMDI) and an isospin-dependent Boltzmann-Uehling-Uhlenbeck (IBUU) transport model, we have studied the effect of the slope parameter  $L$  of the nuclear symmetry energy and the isovector nucleon effective mass  $m_v^*$  on the centroid energy  $E_{-1}$  of the isovector giant dipole resonance (IVGDR) and the electric dipole polarizability  $\alpha_D$  in  $^{208}\text{Pb}$ . We found that both  $E_{-1}$  and  $\alpha_D$  are almost linearly correlated with  $L$  and  $m_v^*$ . With a given isoscalar nucleon effective mass, we are able to constrain the values of  $L$  and  $m_v^*$  with the available experimental data of  $E_{-1}$  and  $\alpha_D$ . From the isoscalar nucleon effective mass  $m_s^* = 0.7m$  constrained by the empirical optical potential, we obtain a constraint of  $L = 64.29 \pm 11.84(\text{MeV})$  and  $m_v^*/m = 0.710 \pm 0.046$ , resulting in the isospin splitting of the nucleon effective mass within  $(m_n^* - m_p^*)/m = (-0.019 \pm 0.090)\delta$ , with  $\delta$  being the isospin asymmetry of nuclear medium. From the isoscalar nucleon effective mass  $m_s^* = 0.84m$  extracted from the excitation energy of the isoscalar giant quadrupole resonance (ISGQR) in  $^{208}\text{Pb}$ , we obtain a constraint of  $L = 53.85 \pm 10.29(\text{MeV})$  and  $m_v^*/m = 0.744 \pm 0.045$ , resulting in the isospin splitting of nucleon effective mass within  $(m_n^* - m_p^*)/m = (0.216 \pm 0.114)\delta$ . The constraint on the neutron-proton effective mass splitting from both ISGQR and IVGDR in  $^{208}\text{Pb}$  is consistent with that from optical model analyses of nucleon-nucleus elastic scatterings. The uncertainty of the isoscalar nucleon effective mass has hampered our accurate constraint on the neutron-proton effective mass splitting.

#### Acknowledgments

We thank Chen Zhong for maintaining the high-quality performance of the computer facility, and acknowledge helpful communications with Zhen Zhang. JX acknowledges support from the Major State Basic Research Development Program (973 Program) of China under Contract No. 2015CB856904 and No. 2014CB845401, the National Natural Science Foundation of China under Grant No. 11475243 and No. 11421505, the "100-Talent Plan" of Shanghai Institute of Applied Physics under Grant No. Y290061011 and No. Y526011011 from the Chinese Academy of Sciences, the Shanghai Key Laboratory of Particle Physics and Cosmology under Grant No. 15DZ2272100, and the "Shanghai Pujiang Program" under Grant No. 13PJ1410600. LWC acknowledges the Major State Basic Research Development Program (973 Program) in China under Contract No. 2013CB834405 and No. 2015CB856904, the National Natural Science Foundation of China under Grant No. 11275125 and No. 11135011, the "Shu Guang" project supported by Shanghai Municipal Education Commission and Shanghai Education Development Foundation,

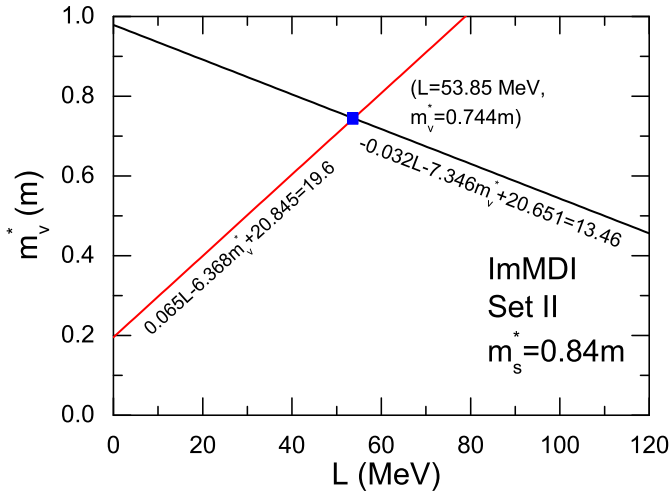


FIG. 6: (Color online) Same as Fig. 4 but with the isoscalar nucleon effective mass  $m_s^* = 0.84m$ .

the Program for Professor of Special Appointment (Eastern Scholar) at Shanghai Institutions of Higher Learning, and the Science and Technology Commission of Shanghai Municipality (11DZ2260700). BAL acknowledges the National Natural Science Foundation of China under Grant No. 11320101004, the U.S. Department of Energy, Office of Science, under Award Number de-sc0013702, and the CUSTIPEN (China-U.S. Theory Institute for Physics with Exotic Nuclei) under the US Department of Energy Grant No. DEFG02-13ER42025. YGM acknowledges the Major State Basic Research Development Program (973 Program) of China under Contract No. 2014CB845401 and the National Natural Science Foundation of China under Contract Nos. 11421505 and 11220101005.

## APPENDIX A. EXPRESSIONS FOR PHYSICS QUANTITIES FROM THE IMMDI INTERACTION

At zero temperature, the phase-space distribution function can be written as  $f_\tau(\vec{r}, \vec{p}) = \frac{2}{h^3} \Theta(p_{f\tau} - p)$ , with  $p_{f\tau} = \hbar(3\pi^2\rho_\tau)^{1/3}$  being the Fermi momentum of nucleons with the isospin label  $\tau$ , and the momentum-dependent part of the single-particle potential as well as that in the potential energy density can be integrated analytically as [71]

$$\begin{aligned} & \int d^3p' \frac{f_\tau(\vec{r}, \vec{p}')}{1 + (\vec{p} - \vec{p}')^2/\Lambda^2} \\ &= \frac{2}{h^3} \pi \Lambda^3 \left\{ \frac{p_{f\tau}^2 + \Lambda^2 - p^2}{2p\Lambda} \ln \left[ \frac{(p + p_{f\tau})^2 + \Lambda^2}{(p - p_{f\tau})^2 + \Lambda^2} \right] \right. \\ &+ \left. \frac{2p_{f\tau}}{\Lambda} - 2 \left( \arctan \frac{p + p_{f\tau}}{\Lambda} - \arctan \frac{p - p_{f\tau}}{\Lambda} \right) \right\} \end{aligned} \quad (\text{A.23})$$

and

$$\begin{aligned} & \int \int d^3p d^3p' \frac{f_\tau(\vec{r}, \vec{p}) f_{\tau'}(\vec{r}, \vec{p}')}{1 + (\vec{p} - \vec{p}')^2/\Lambda^2} \\ &= \frac{1}{6} \left( \frac{4\pi}{h^3} \right)^2 \Lambda^2 \{ p_f(\tau) p_f(\tau') [3(p_{f\tau}^2 + p_{f\tau'}^2) - \Lambda^2] \\ &+ 4\Lambda \left[ (p_{f\tau}^3 - p_{f\tau'}^3) \arctan \left( \frac{p_{f\tau} - p_{f\tau'}}{\Lambda} \right) \right. \\ &- \left. (p_{f\tau}^3 + p_{f\tau'}^3) \arctan \left( \frac{p_{f\tau} + p_{f\tau'}}{\Lambda} \right) \right] \\ &+ \frac{1}{4} [\Lambda^4 + 6\Lambda^2(p_{f\tau}^2 + p_{f\tau'}^2) - 3(p_{f\tau}^2 - p_{f\tau'}^2)^2] \\ &\times \left. \ln \left[ \frac{(p_{f\tau} + p_{f\tau'})^2 + \Lambda^2}{(p_{f\tau} - p_{f\tau'})^2 + \Lambda^2} \right] \right\}. \end{aligned} \quad (\text{A.24})$$

The binding energy per nucleon for asymmetric nuclear matter can be expressed as

$$E(\rho, \delta) = \frac{V(\rho, T=0, \delta)}{\rho} + E_k(\rho, \delta) \quad (\text{A.25})$$

with the kinetic energy per nucleon calculated from

$$\begin{aligned} E_k(\rho, \delta) &= \frac{1}{\rho} \int d^3p \left[ \frac{p^2}{2m} f_n(\vec{r}, \vec{p}) + \frac{p^2}{2m} f_p(\vec{r}, \vec{p}) \right] \\ &= \frac{4\pi}{5mh^3\rho} (p_{fn}^5 + p_{fp}^5), \end{aligned} \quad (\text{A.26})$$

where  $p_{fn(p)} = \hbar(3\pi^2\rho_{n(p)})^{1/3}$  is the Fermi momentum of neutrons (protons), and  $m$  is the nucleon mass.

By setting  $\rho_n = \rho_p = \frac{\rho}{2}$  and  $p_{fn} = p_{fp} = p_f$ , we can express the binding energy per nucleon for symmetric nuclear matter as [71]

$$\begin{aligned} E_0(\rho) &= \frac{8\pi}{5mh^3\rho} p_f^5 + \frac{\rho}{4\rho_0} (A_l + A_u) + \frac{B}{\sigma+1} \left( \frac{\rho}{\rho_0} \right)^\sigma \\ &+ \frac{1}{3\rho_0\rho} (C_l + C_u) \left( \frac{4\pi}{h^3} \right)^2 \Lambda^2 \\ &\times \left[ p_f^2 (6p_f^2 - \Lambda^2) - 8\Lambda p_f^3 \arctan \left( \frac{2p_f}{\Lambda} \right) \right. \\ &+ \left. \frac{1}{4} (\Lambda^4 + 12\Lambda^2 p_f^2) \ln \left( \frac{4p_f^2 + \Lambda^2}{\Lambda^2} \right) \right]. \end{aligned} \quad (\text{A.27})$$

The saturation density is determined by the zero point of the first-order derivative of the binding energy per nucleon, with the latter expressed as [71]

$$\begin{aligned} & \frac{dE_0(\rho)}{d\rho} \\ &= \frac{16\pi}{15mh^3\rho^2} p_f^5 + \frac{1}{4\rho_0} (A_l + A_u) + \frac{B\sigma}{\sigma+1} \frac{\rho^{\sigma-1}}{\rho_0^\sigma} \\ &+ \frac{1}{3\rho_0\rho^2} (C_l + C_u) \left( \frac{4\pi}{h^3} \right)^2 \Lambda^2 \\ &\times \left[ 2p_f^4 + \Lambda^2 p_f^2 - \frac{1}{4} (\Lambda^4 + 4\Lambda^2 p_f^2) \ln \left( \frac{4p_f^2 + \Lambda^2}{\Lambda^2} \right) \right]. \end{aligned} \quad (\text{A.28})$$

The incompressibility of symmetric nuclear matter is defined as  $K_0 = 9\rho_0^2(d^2E_0/d\rho^2)_{\rho=\rho_0}$ , with the second-order derivative of the binding energy per nucleon expressed as [71]

$$\begin{aligned} & \frac{d^2E_0(\rho)}{d\rho^2} \\ &= -\frac{16\pi}{45mh^3\rho^3} p_f^5 + \frac{B\sigma(\sigma-1)}{\sigma+1} \frac{\rho^{\sigma-2}}{\rho_0^\sigma} \\ &+ \frac{2}{3\rho_0\rho^3} (C_l + C_u) \left( \frac{4\pi}{h^3} \right)^2 \Lambda^2 \\ &\times \left[ -\frac{2}{3} p_f^4 - \Lambda^2 p_f^2 + \Lambda^2 \left( \frac{\Lambda^2}{4} + \frac{2}{3} p_f^2 \right) \ln \left( \frac{4p_f^2 + \Lambda^2}{\Lambda^2} \right) \right]. \end{aligned} \quad (\text{A.29})$$



The symmetry energy by definition can be written as [71]

$$\begin{aligned}
& E_{\text{sym}}(\rho) \\
&= \frac{1}{2} \left( \frac{\partial^2 E}{\partial \delta^2} \right)_{\delta=0} \\
&= \frac{8\pi}{9mh^3} p_f^5 + \frac{\rho}{4\rho_0} (A_l - A_u) - \frac{Bx}{\sigma + 1} \left( \frac{\rho}{\rho_0} \right)^\sigma \\
&+ \frac{C_l}{9\rho_0\rho} \left( \frac{4\pi}{h^3} \right)^2 \Lambda^2 \left[ 4p_f^4 - \Lambda^2 p_f^2 \ln \left( \frac{4p_f^2 + \Lambda^2}{\Lambda^2} \right) \right] \\
&+ \frac{C_u}{9\rho_0\rho} \left( \frac{4\pi}{h^3} \right)^2 \Lambda^2 \left[ 4p_f^4 - p_f^2 (4p_f^2 + \Lambda^2) \ln \left( \frac{4p_f^2 + \Lambda^2}{\Lambda^2} \right) \right]. \quad (\text{A.30})
\end{aligned}$$

The slope parameter of the symmetry energy at the saturation density is defined as  $L = 3\rho_0 [dE_{\text{sym}}(\rho)/d\rho]_{\rho=\rho_0}$ , with the first-order derivative of the symmetry energy expressed as [71]

$$\begin{aligned}
& \frac{dE_{\text{sym}}(\rho)}{d\rho} \\
&= \frac{16\pi}{27mh^3\rho^2} p_f^5 + \frac{1}{4\rho_0} (A_l - A_u) \\
&- \frac{Bx\sigma}{\sigma + 1} \frac{\rho^{\sigma-1}}{\rho_0^\sigma} + \frac{C_l + C_u}{27\rho_0\rho^2} \left( \frac{4\pi}{h^3} \right)^2 \Lambda^2 \\
&\times \left[ 4p_f^4 + \Lambda^2 p_f^2 \ln \left( \frac{4p_f^2 + \Lambda^2}{\Lambda^2} \right) - \frac{8\Lambda^2 p_f^4}{4p_f^2 + \Lambda^2} \right] \\
&- \frac{4C_u}{27\rho_0\rho^2} \left( \frac{4\pi}{h^3} \right)^2 \Lambda^2 p_f^4 \left[ \ln \left( \frac{4p_f^2 + \Lambda^2}{\Lambda^2} \right) + \frac{8p_f^2}{4p_f^2 + \Lambda^2} \right]. \quad (\text{A.31})
\end{aligned}$$

The isoscalar nucleon effective mass  $m_s^*$  is defined as the nucleon effective mass in symmetric nuclear matter at the saturation density, and it can be calculated from

the mean-field potential  $U_0$  in symmetric nuclear matter via

$$m_s^* = m \left( 1 + \frac{m}{p} \frac{dU_0}{dp} \right)_{p=p_f}^{-1}. \quad (\text{A.32})$$

In asymmetric nuclear matter, the isovector nucleon effective mass can be calculated through the following relation

$$\frac{\hbar^2}{2m_{n(p)}^*} = \frac{2\rho_{n(p)}}{\rho_0} \frac{\hbar^2}{2m_s^{*2}} + \left( 1 - \frac{2\rho_{n(p)}}{\rho_0} \right) \frac{\hbar^2}{2m_v^*}, \quad (\text{A.33})$$

with the neutron (proton) effective mass defined as

$$m_{n(p)}^* = m \left( 1 + \frac{m}{p} \frac{dU_{n(p)}}{dp} \right)_{p=p_f}^{-1}. \quad (\text{A.34})$$

Keeping the first-order term of the isospin asymmetry  $\delta$ , the neutron-proton effective mass splitting is related to the isoscalar and isovector effective mass through the following relation

$$m_n^* - m_p^* \approx \frac{2m_s^*}{m_v^*} (m_s^* - m_v^*) \delta. \quad (\text{A.35})$$

Finally, the mean-field potential of a nucleon with infinitely large momentum in symmetric nuclear matter at the saturation density can be expressed as

$$U_0^\infty = \frac{A_l + A_u}{2} + B. \quad (\text{A.36})$$

The values of the parameters  $A_0$ ,  $B$ ,  $C_{u0}$ ,  $C_{l0}$ ,  $\sigma$ ,  $\Lambda$ ,  $x$ , and  $y$  can be obtained from Eqs. (A.27-A.36), with given  $\rho_0$ ,  $E_0(\rho_0)$ ,  $K_0$ ,  $U_0^\infty$ ,  $m_s^*$ ,  $E_{\text{sym}}(\rho_0)$ ,  $L$ , and  $m_v^*$ .

- 
- [1] B.A. Li, C.M. Ko, and W. Bauer, *Int. J. Mod. Phys. E* **7**, 147 (1998).  
[2] *Isospin Physics in Heavy-Ion Collisions at Intermediate Energies*, Eds. B.A. Li and W. Uuo Schröder (Nova Science Publishers, Inc, New York, 2001).  
[3] P. Danielewicz, R. Lacey, and W.G. Lynch, *Science* **298**, 1592 (2002).  
[4] V. Baran, M. Colonna, V. Greco, and M. Di Toro, *Phys. Rep.* **410**, 335 (2005).  
[5] A.W. Steiner, M. Prakash, J.M. Lattimer, and P.J. Ellis, *Phys. Rep.* **411**, 325 (2005).  
[6] J.M. Lattimer and M. Prakash, *Phys. Rep.* **442**, 109 (2007).  
[7] B.A. Li, L.W. Chen, and C.M. Ko, *Phys. Rep.* **464**, 113 (2008).  
[8] B.A. Li, À. Ramos, G. Verde, and I. Vidaña, *Topical issue on nuclear symmetry energy*, *Eur. Phys. J. A* **50**, No.2 (2014).  
[9] L.W. Chen, arXiv:1212.0284 [nucl-th].  
[10] B.A. Li and X. Han, *Phys. Lett. B* **727**, 276 (2013).  
[11] M. Oertel, M. Hempel, T. Klähn, and S. Typel, arXiv:1610.03361 [astro-ph.HE].  
[12] B.A. Li, *Phys. Rev. C* **69**, 064602 (2004).  
[13] J. Rizzo, M. Colonna, and M. Di Toro, *Phys. Rev. C* **72**, 064609 (2005).  
[14] V. Giordano *et al.*, *Phys. Rev. C* **81**, 044611 (2010).  
[15] Z.Q. Feng, *Phys. Rev. C* **84**, 024610 (2011).  
[16] Z.Q. Feng, *Nucl. Phys. A* **878**, 3 (2012).  
[17] Y.X. Zhang, M.B. Tsang, Z.X. Li, and H. Liu, *Phys. Lett. B* **732**, 186 (2014).  
[18] W.J. Xie and F.S. Zhang, *Phys. Lett. B* **735**, 250 (2014).  
[19] H.Y. Kong, Y. Xia, J. Xu, L.W. Chen, B.A. Li, and Y.G. Ma, *Phys. Rev. C* **91**, 047601 (2015).  
[20] L. Ou *et al.*, *Phys. Lett. B* **697**, 246 (2011).  
[21] J. Xu, L.W. Chen, and B.A. Li, *Phys. Rev. C* **91**, 014611 (2015).  
[22] C. Xu, B.A. Li, and L.W. Chen, *Phys. Rev. C* **82**, 054607 (2010).  
[23] B.A. Li and L.W. Chen, *Mod. Phys. Lett. A* **30**, 1530010 (2015); B.A. Li, B.J. Cai, L.W. Chen, and X.H. Li, Nu-

- clear Science and Techniques, **27**, 141 (2016).
- [24] J. Blaizot *et al.*, Nucl. Phys. A **591**, 435 (1995).
  - [25] D.H. Youngblood, H.L. Clark, and Y.W. Lui, Phys. Rev. Lett. **82**, 691 (1999).
  - [26] B. K. Agrawal, S. Shlomo, and V. Kim Au, Phys. Rev. C **68**, 031304 (2003).
  - [27] G. Colò *et al.*, Phys. Rev. C **70**, 024307 (2004).
  - [28] B.G. Todd-Rutel and J. Piekarewicz, Phys. Rev. Lett. **95**, 122501 (2005).
  - [29] A. Bohr and B.R. Mottelson, *Nuclear Structure*, Vols. I and II (W. A. Benjamin Inc., Reading, MA, 1975).
  - [30] O. Bohigas, A.M. Lane, and J. Martorell, Phys. Rep. **51**, 267 (1979).
  - [31] J.-P. Blaizot, Phys. Rep. **64**, 171 (1980).
  - [32] P. Klüpfel, P.-G. Reinhard, T.J. Bürvenich, and J.A. Maruhn, Phys. Rev. C **79**, 034310 (2009).
  - [33] X. Roca-Maza *et al.*, Phys. Rev. C **87**, 034301 (2013).
  - [34] Z. Zhang and L.W. Chen, Phys. Rev. C **93**, 034335 (2016).
  - [35] A. Klimkiewicz *et al.*, Phys. Rev. C **76**, 051603(R) (2007).
  - [36] L. Trippa, G. Colò, and E. Vigezzi, Phys. Rev. C **77**, 061304(R) (2008).
  - [37] A. Carbone *et al.*, Phys. Rev. C **81**, 041301(R) (2010).
  - [38] P.-G. Reinhard and W. Nazarewicz, Phys. Rev. C **81**, 051303(R) (2010).
  - [39] A. Tamii *et al.*, Phys. Rev. Lett. **107**, 062502 (2011).
  - [40] J. Piekarewicz, B.K. Agrawal, G. Colò, W. Nazarewicz, N. Paar, P.-G. Reinhard, X. Roca-Maza, and D. Vretenar, Phys. Rev. C **85**, 041302(R) (2012).
  - [41] X. Roca-Maza, G. Pozzi, M. Brenna, K. Mizuyama, and G. Colò, Phys. Rev. C **85**, 024601 (2012).
  - [42] D. Vretenar, Y.F. Niu, N. Paar, and J. Meng, Phys. Rev. C **85**, 044317 (2012).
  - [43] V. Baran, B. Frecus, M. Colonna, and M. Di Toro, Phys. Rev. C **85**, 051601(R) (2012).
  - [44] X. Roca-Maza, M. Brenna, G. Colò, M. Centelles, X. Viñas, B.K. Agrawal, N. Paar, D. Vretenar, and J. Piekarewicz, Phys. Rev. C **88**, 024316 (2013).
  - [45] C. Tao *et al.*, Phys. Rev. C **87**, 014621 (2013); C. Tao *et al.*, Nuclear Science and Techniques, **24**, 030502 (2013).
  - [46] G. Colò, U. Garg, and H. Sagawa, Eur. Phys. J. A **50**, 26 (2014).
  - [47] X. Roca-Maza, X. Viñas, M. Centelles, B.K. Agrawal, G. Colò, N. Paar, J. Piekarewicz, and D. Vretenar, Phys. Rev. C **92**, 064304 (2015).
  - [48] Z. Zhang and L.W. Chen, Phys. Rev. C **93**, 031301(R) (2015).
  - [49] H. Zheng, S. Burrello, M. Colonna, and V. Baran, Phys. Rev. C **94**, 014313 (2016).
  - [50] V. Baran, D.M. Brink, M. Colonna, and M. Di Toro, Phys. Rev. Lett. **87**, 182501 (2001).
  - [51] V. Baran, M. Cabibbo, M. Colonna, M. Di Toro, and N. Tsoneva, Nucl. Phys. A **679**, 373 (2001).
  - [52] M. Papa *et al.*, Phys. Rev. C **72**, 064608 (2005).
  - [53] V. Baran, C. Rizzo, M. Colonna, M. Di Toro, and D. Pierrousakou, Phys. Rev. C **79**, 021603(R) (2009).
  - [54] H.L. Wu *et al.*, Phys. Rev. C **81**, 047602 (2010).
  - [55] S.Q. Ye *et al.*, Phys. Rev. C **88**, 047602 (2013); S.Q. Ye *et al.*, Nuclear Science and Techniques, **25**, 030501 (2014).
  - [56] C.B. Das, S. Das Gupta, C. Gale, and B.A. Li, Phys. Rev. C **67**, 034611 (2003).
  - [57] L.W. Chen, C.M. Ko, and B.A. Li, Phys. Rev. Lett. **94**, 032701 (2005).
  - [58] L.W. Chen, C.M. Ko, B.A. Li, C. Xu, and J. Xu, Eur. Phys. J. A **50**, 29 (2014).
  - [59] S.S. Dietrich and B.L. Berman, At. Data Nucl. Data Tables **38**, 199 (1988).
  - [60] J. Xu and C.M. Ko, Phys. Rev. C **82**, 044311 (2010).
  - [61] M. Urban, Phys. Rev. C **85**, 034322 (2012).
  - [62] S. Hama *et al.*, Phys. Rev. C **41**, 2737 (1990).
  - [63] E.D. Cooper *et al.*, Phys. Rev. C **47**, 297 (1993).
  - [64] S.K. Patra *et al.*, Nucl. Phys. A **703**, 240 (2002).
  - [65] M. Buenerd, J. Phys. Colloques **45**, C4-115 (1984); D.H. Youngblood, P. Bogucki, J.D. Bronson, U. Garg, Y. W. Lui, and C.M. Rozsa, Phys. Rev. C **23**, 1997 (1981); S. Brandenburg, Ph.D. thesis, University of Groningen, 1985; D.H. Youngblood, Y.-W. Lui, H.L. Clark, B. John, Y. Tokimoto, and X. Chen, Phys. Rev. C **69**, 034315 (2004).
  - [66] S. Habib *et al.*, Phys. Rev. D **76**, 083503 (2007).
  - [67] F.A. Gómez *et al.*, The Astrophysical Journal **760**, 112 (2012).
  - [68] S. Pratt *et al.*, Phys. Rev. Lett. **114**, 202301 (2015).
  - [69] E. Sangaline and S. Pratt, Phys. Rev. C **93**, 024908 (2016).
  - [70] X.H. Li *et al.*, Phys. Lett. B **743**, 408 (2015).
  - [71] J. Xu, L.W. Chen, B.A. Li, and H.R. Ma, The Astrophysical Journal **697**, 1549 (2009); J. Xu, Ph.D. thesis, Shanghai Jiao Tong University.